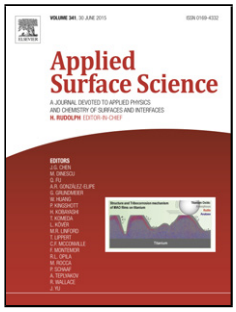

Title: Anisotropic Ni-Fe-B Films with Varying Alloy Composition for High Frequency Magnetics on Silicon Applications

Author: Ricky Anthony Brian J. Shanahan Finbarr Waldron Cian Ó. Mathúna James F. Rohan

PII: S0169-4332(15)02116-9
DOI: http://dx.doi.org/doi:10.1016/j.apsusc.2015.09.025
Reference: APSUSC 31239

To appear in: *APSUSC*

Received date: 15-5-2015
Revised date: 31-8-2015
Accepted date: 1-9-2015

Please cite this article as: R. Anthony, B.J. Shanahan, F. Waldron, C.Ó. Mathúna, J.F. Rohan, Anisotropic Ni-Fe-B Films with Varying Alloy Composition for High Frequency Magnetics on Silicon Applications, *Applied Surface Science* (2015), http://dx.doi.org/10.1016/j.apsusc.2015.09.025

Highlights

A CMOS compatible electroless Ni-Fe deposition process is shown

Anisotropic nanocrystalline Ni-Fe films deposited in an external magnetic field

Magnetic and electrical data demonstrate high frequency capabilities

Film composition and characteristics modified at reduced deposition temperature

Film composition tailored over wide range by changing DMAB concentration

Desirable magnetic and electrical characteristics achieved by varying Fe content

A simpler alternative to electroplated films for magnetics applications

Anisotropic Ni-Fe-B Films with Varying Alloy Composition for High Frequency Magnetics on Silicon Applications

Ricky Anthony, Brian J. Shanahan, Finbarr Waldron, Cian Ó Mathúna and James F. Rohan*

Tyndall National Institute, University College Cork, Lee Maltings, Cork, Ireland

*Corresponding Author: james.rohan@tyndall.ie

1. Introduction:

In the last two decades soft magnetic materials with high permeability (μ), high resistivity (□), low coercivity (H_c) and high saturation flux density (B_{sat}) have been intensively studied for various silicon integrated applications such as inductors [1-3], transformers [4-5], motors [6] and recording heads [7]. For these applications Ni-Fe alloys have been the most accepted material based on high saturation flux density (<1.5 T), high resistivity (20-45 μΩ-cm) and lower coercivity (<1 Oe) depending on alloy composition. However, Ni-Fe films grown with physical vapour deposition (PVD) techniques result preferentially in columnar growth [8-9] for films greater than 180 nm in thickness. This results in an undesirable tenfold increase in coercivity. Electrochemical processing of Ni-Fe alloys and layer by layer deposition eliminates the columnar growth issue. Electrochemical deposition of magnetic films is also a faster process for soft magnetic films such as NiFe (81/19) [10-11], NiFe (45/55) [12] and CoNiFe [13-16].

A significant issue for passive magnetic components such as micro-inductors and micro-transformers on silicon is the reduced efficiency due to losses from both the copper windings and the magnetic core [19-20]. The core suffers from hysteresis and eddy current losses. High coercivity materials increase the overall hysteresis loss whereas high conductivity materials make the core susceptible to eddy current losses. For

high frequency operation (up to 100 MHz), the devices require core materials with high anisotropy along the hard axis which prevents the core from saturating during high frequency operation. As a result $Ni_{45}Fe_{55}$ is preferred for its high saturation flux density (1.5 T) and resistivity (45 μOhm-cm) and $Ni_{80}Fe_{20}$ for its lower coercivity (< 0.5 Oe). This trade-off between magnetic and electrical properties remains a major challenge in electroplated films. A deposition process wherein the Fe composition can be altered readily depending upon application is therefore highly desirable.

Electroless processing has a number of advantages by comparison with electrolytic deposition. Conformal homogeneous deposits with high yield in high aspect ratio structures and in three dimensional topologies without full or highly conducting seed layers are achievable [21]. This process is ideal for nanowires growth [22-24], deposition in through silicon vias [25] and can result in less porous films [26] than those achieved with electrolytic deposition. A tertiary current distribution characteristic is another issue leading to non-uniformity in electrolytic films [27] that can require complex and costly anode placement. For DMAB based electroless deposition the nanocrystalline structure of the resulting deposits leads to a higher saturation flux density (B_{Sat}) by comparison with hypophosphite based baths [16]. This is due to the lower codeposit content of boron from DMAB (~ 1%) than phosphorus from hypophosphite (~ 7%) baths which deteriorates the magnetic properties.

In this work DMAB was used to achieve high saturation flux density and low coercivity. The deposition was performed in the presence of an external magnetic field (>300 Oe) to achieve high anisotropy through preferential orientation of the magnetic dipoles during deposition. Secondly, we report that high DMAB concentration leads to preferable Fe deposition at lower deposition temperatures, when other parameters are kept constant. This contributes to an increase in resistivity with excellent magnetic properties. The target of the work was to achieve high quality magnetic films with the following specific characteristics from a CMOS compatible plating solution to assist with integration of the magnetic devices on silicon:

Low coercivity (< 0.5 Oe)

High resistivity (> 25 μΩ-cm)

High anisotropy field (> 10 Oe along hard axis)

Saturation flux density (> 1T)

2. Experimental Procedure:

All the solutions were prepared from de-ionized (DI) water of resistivity 18 MΩ-cm. The chemicals used were purchased from Sigma-Aldrich and used as received. The electroless process was performed in glass beakers. The temperature of the bath was maintained with an Ikamag RCT stirring hotplate and IKA H60 temperature probe. The pH was monitored with an OAKTON pH 6 (Acorn series) and adjusted with ammonium hydroxide solution. Silicon (100) wafers were sputtered with 20 nm Ti for adhesion followed by 100 nm Cu in Nordiko DC magnetron sputtering system. Commercially available positive tone photoresist AZ9260 (Microchemicals GmbH) is used to pattern the wafers. Magnetic films were deposited in the presence of a magnetic field (>300 Oe).

The morphology and composition of the deposits were analysed with a Quanta FEG600 scanning electron microscope (SEM) with energy dispersive X-rays (EDX). Intensity correction for trace elements was performed. Film thickness was confirmed with a Tencor (P-10) surface profilometer. The static magnetic properties were analysed with a BH loop tracer (MESA HF200P, SHB instruments). The coercivity (H_c), saturation flux density (B_{sat}) and anisotropy field (H_k) values were obtained from the BH loops of the

samples. Complex permeability characterization at room temperature were performed with a wide-band (1MHz to 9 GHz) permeameter (PMM 9G, Ryowa Electronics). The electrical resistivities of the samples were measured with a four-point probe system. The currents (I) and voltages (V) across the sample were measured with an Agilent DC multimeter and the resistivity calculated as: □=K (V*T/I), where K is correction factor (~4.53 in this case) and T is thickness of the plated material. Microstructural X-ray diffraction (XRD) analyses of $Ni_{81}Fe_{19}$ (permalloy) and $Ni_{37}Fe_{63}$ films were performed on a PANalytical X'Pert PRO MPD XRD system equipped with Cu K-alpha radiation (1.5405 Å) source and goniometer resolution of 0.001^0. Grain sizes and lattice orientation where determined from the XRD results obtained.

3. Results and Discussions:

Deposition rate and alloy composition

$Ni_{81}Fe_{19}$ films were deposited electrolessly in the presence of a magnetic field. The pH of the bath was adjusted to 6.5 with diluted ammonium hydroxide, while the deposition temperature was maintained at 75 ^oC. All the bath constituents were solubilised before adding DMAB. Table I lists the bath compositions to achieve different Ni-Fe alloys where bath-II is the composition for uniform permalloy deposition. Thin films with thickness from 330 nm to ~1.58 µm were deposited to estimate the deposition rate. Fig. 1(a) shows the deposition rate of permalloy films deposited under these conditions. The initial plating rate was ~ 6.6 µm/hr decreasing gradually to 3.1 µm/hr after 10 minutes of plating. The Ni and Fe contents were found to be 78%-81% and 22%-19% respectively by EDX, with negligible boron content measured (< 1%) in all the deposited films. This deposition process is found to be reproducible with consistent results. Fig. 1(b) depicts the SEM cross-section micrograph of uniform film cross-sections with thickness of 770 nm and 1.58 µm. All the films were deposited in a strong magnetic field, > 300 Oe provided by NdFeB magnets. The distance between the magnets and the substrate plays a significant role in determining the anisotropy of films. Hence the distance between the two magnets and substrate was maintained at 15 cm. Deposition in a magnetic field has been reported for CoNiFe films [31-33], but no comprehensive study has been done on electroless Ni-Fe alloy deposition in magnetic field.

Further optimisation of the deposition was investigated with increased metal ion content (Ni and Fe ions) while maintaining the Ni and Fe ratio at 1:1 and the other constituents unchanged. Fig. 2 shows that higher Ni and Fe content in the bath increases the deposition rate. However, as observed from the figure, this increase in deposition rate reaches a plateau as the Ni salt concentration increases above 0.12 mol-dm^{-3}. There is no significant change in composition on increasing the metal ion concentration with deposits in the range Ni (74-81) and Fe (26-19) at. wt. %. This increase in deposition rate can be attributed to higher catalytic activity at the Ni for the oxidation reaction of DMAB. This is consistent with electrolessly deposited Ni-Co alloys reported in literature [14, 16, 37]. For the remainder of the processing a Ni content of 0.06 mol-dm^{-3} was utilised.

Electroless deposition of Ni-Fe alloys [34-36] from hypophosphite baths has also been reported previously. These baths can provide up to 25 % Fe composition [34]. Wang et al [36] has reported deposition of Ni-Fe-P amorphous films from boric acid and sodium citrate baths to achieve 20% Fe and 10% Ni. The film quality and grain size strongly depends on the complexing additives and reducing agent. However, in this work, diammonium citrate and lactic acid were employed as complexing agents and DMAB was used as

reducing agent as similar bath compositions by the authors have shown excellent nanocrystalline CoNiFe-B thin films [16]. For magnetic devices on silicon it is essential to have Fe rich deposits. A higher Fe content offers an increase in resistivity and saturation flux density with augmented coercivity. Lower coercivity is another vital parameter to reduce magnetic core losses in micro-inductors and transformers. To achieve this, a trade-off exists in terms of the magnetic and electrical properties of the Ni-Fe alloy films which can be probed by varying the Ni and Fe compositions.

Higher DMAB content can increase Fe content relative to Co in CoNiFe-B deposits [15]. To achieve this in Ni-Fe alloys the DMAB concentration was increased from 0.017 to 0.136 mol-dm^{-3}. Fig. 3 shows the influence of DMAB content on the deposition temperature. It is observed that increasing the DMAB content permitted film deposition at much lower temperatures. A significant increase in deposition rate is also observed from ~ 6 to ~ 12.5 µm/hr. Fig. 4 shows the surface morphology of the deposited films at 0.017, 0.034, 0.102 and 0.136 mol-dm^{-3} DMAB concentrations. These deposited samples were prepared at 85 ^{0}C, 75 ^{0}C, 65 ^{0}C and 58 ^{0}C respectively. It is found that deposits with 63% Fe content can be achieved at lower temperatures. Fig.5 shows the deposited Ni and Fe content at different DMAB concentrations.

The photoresist used in the process (AZ 9260) is compatible with microelectromechanical processing. The magnetic core thickness (770 nm - 1.58 µm) in micro-inductors and transformers is chosen based on the frequency of operation (20 -100 MHz) such that eddy current losses can be kept minimum. In the case of electroplated magnetic films deposits at the edge of the wafer closer to the electrical contact can result in thicker a core which increase the core losses and reduces the overall efficiency of the devices at the edge of the wafer. Moreover, the deposition rates of electroplated cores deposited under pulse reverse plating conditions has been optimised to ~ 3 µm/hr by comparison with 6.6 µm/hr reported in this work without compromising on magnetic characteristics.

Magnetic properties

An increase in converter switching frequencies has enabled miniaturization of passive devices like inductors and transformers. However, to achieve high inductance in limited footprints (<2 mm^2) without reducing efficiency a soft magnetic core is critical. A magnetic core increases the flux confinement thereby increasing the inductance in a stipulated footprint. A magnetic core with higher coercivity will escalate the overall losses. Hence, magnetic cores should be highly anisotropic in nature with distinct easy (EA) and hard axes (HA). Along the hard axis, the coercivity should be lower and saturate at a higher external field. In this work high anisotropy has been achieved by depositing the films in an external NdFeB magnetic field (> 300 Oe).

The deposited films were investigated for their magnetic properties using a BH loop tracer. 100 Oe external fields were applied to completely saturate the sample during measurement. Fig. 6 (a) shows the easy and hard axes of the electrolessly deposited permalloy film ($Ni_{81}Fe_{19}$) in bath I. The saturation flux density was measured to be ~1 T. The H_k values for the permalloy films increased from 12 Oe to 14 Oe depending on thicknesses deposited while the HA coercivity decreased with thickness and the coercivity values were < 0.48 Oe with 0.37 Oe being the minimum value attained. Fig. 6 (b) shows the EA and HA of a $Ni_{37}Fe_{63}$ sample deposited in the external magnetic field. The sample exhibited a high B_{sat} value ~1.75 T with the high coercivity value ~1.2 Oe attributed to higher Fe content. The composition to be used is based on the trade-off in performance and is therefore determined by the application. It is possible to achieve various Fe compositions (between 19-63%) by keeping the same electroless bath composition and changing DMAB concentration only. Fig. 7 shows the anisotropy field and coercivity values obtained

versus film thickness. The coercivity decreases with an increase in thickness (d). This is in accordance with Ne´els equation [38]: H_c (coercivity) = Ld^{-n}, where L and n are constants depending on magnetization of the films, energy wall domain, structure, thickness uniformity and surface geometry. The anisotropy in the films increases with thickness which is well established [39]. This is also influenced by external magnetic field and roughness in the films.

There have been very few reports on high frequency characteristics of electroless magnetic materials and in particular Ni-Fe alloys. Hence, it important to assess the high frequency response of electroless Ni-Fe alloys for their applicability in high frequency integrated magnetics. Fig. 8 (a) and (b) depict the real and imaginary permeability response of $Ni_{81}Fe_{19}$ films of different thickness at 20 Oe external bias. As observed from the figure, the permeability is stable beyond 100 MHz and has a roll-off frequency of ~ 200 MHz with significant increase in the cut-off frequency for the 1.58 μm thick deposit. This can be attributed to high anisotropy (~14 Oe) of the deposited film. The decrease in permeability with thickness is in accordance with previously reported works [39-40]. The imaginary permeability (fig. 8 (b)) is a measure of loss in the material. It can also be seen that the film has low imaginary permeability for thicker deposits, showing the contribution to large anisotropy of increasing film thickness.

Resistivity

The electrical resistivity of the material is a significant parameter on which the critical thickness of the magnetic core is based. This thickness is estimated from the skin depth equation given by:

$$d = \sqrt{\frac{\rho}{f * \mu_0 \mu_r * \pi}} \qquad (1)$$

Where, □, $\mu_0\mu_r$ and f are the resistivity, permeability of the film and the frequency of operation. For core thicknesses > d, eddy current losses contribute to the core loss. Thicker cores on the other hand allow better flux confinement in the cores which in turn increases the inductance density. Hence it is desirable to have highly resistive magnetic films without degrading the magnetic properties. Increasing the resistivity through co-deposition of phosphorus [16] or with diethylenetriamine (DETA) [13] have been reported previously. However, deposition in hypophosphite baths result in higher coercivity values [16]. In this work DMAB baths were preferred over hypophosphite baths for lower coercivity. Hence, to increase the resistivity of the deposits the Ni content was gradually decreased (81%-37%) by varying DMAB content in the bath (as listed in Table I) to achieve a higher Fe content. As seen in fig.9, ~ 63 μOhm-cm resistivity with $Ni_{37}Fe_{63}$ films is achieved for bath V.

Micro-structural Analysis

XRD analysis was performed to understand the cause of the low film coercivity. It is well established that small grain sizes result in low coercivity films [40-41]. Yi et. al. [42] has shown that smoothness of the underlying substrate influences the grain size of the deposited film. Fig. 10 shows the XRD peaks obtained from $Ni_{81}Fe_{19}$ and $Ni_{37}Fe_{63}$ electroless films which did not yield any significant peaks other than those from the magnetic film. There is a shift in the peak as Fe% increases from 19% to 63%. This shift is attributed to the change in BCC rich phase ($Ni_{81}Fe_{19}$) at peak 43.45^0 to a mixed FCC-BCC ($Ni_{37}Fe_{63}$) phase at peak

43.35^0 with higher BCC phase. The grain sizes calculated for $Ni_{37}Fe_{63}$ and $Ni_{81}Fe_{19}$ films using the well-established Debye-Scherrer formula indicates grain sizes of 30 nm and 32.4 nm, respectively. These values are well within the nano-crystalline range and are the basis for the lower coercivities in these films..

Conclusions

An electroless nickel-iron alloy deposition process utilising an external magnetic field has been described to achieve varying nickel and iron compositions for the specific high frequency application range. High anisotropy, low coercivity and high saturation flux density values were achieved which show significant improvements appropriate for high frequency magnetics on silicon applications. It has been shown that higher Fe content films (from 19 to ~ 63%) can be achieved by increasing the DMAB concentration. The magnetic, electrical and structural characteristics of these application specific films with different Fe content were reported. The coercivity values ranging from 0.37 to 1.2 Oe, saturation flux density from 1 - 1.75 T and resistivity values with 28 to 63 µOhm-cm have been obtained depending on film composition. The increased resistivity of the films reduces the eddy current losses whereas the permeability studies suggests high frequency applicability (>100 MHz) of the thin films as core material in magnetics on Si applications. The micro-structural analyses suggested that the deposits are nano-crystalline in nature with grain sizes below < 33 nm resulting in low coercivity values in the films. The pH value (~6.5) is compatible with standard photoresists (e.g. AZ9260, SU-8, THB-151N) used in silicon based microfabrication processes. In conclusion, the electroless Ni-Fe alloy deposition process developed provides excellent magnetic and electrical properties which can be employed as core materials in the fabrication of silicon integrated inductors and transformers.

Acknowledgement

The authors wish to acknowledge Central Fabrication Facilities (CFF), Tyndall National Institute and European Union for funding the work through FP-7 under the project ‘PowerSwipe’ (Grant no.: 318529).

References

S. Prabhakaran, T. O’Donnell, C.R. Sullivan, M. Brunet, S. Roy, C. Ó Mathúna, Microfabricated coupled inductors for integrated power converter, J. Magn. Magn. Mater., 290-291 (2005) 290-291.

J.F. Rohan, D.P. Casey, J. O’Brien, M. Hegarty, A-M. Kelleher, N. Wang, B. Jamieson, F. Waldron, S. Kulkarni, S. Roy, S.C. Ó Mathúna, Integrated micro-inductors on semiconductor substrates for power supply on chip, ECS Trans., 41(2011) 341-347.

N. Wang, T. O’ Donnell, S. Roy, M. Brunet, P. McCloskey, S.C. Ó Mathúna, High-frequency micro-machined power inductors, J. Magn. Magn. Mater., 290-291 (2005) 1347-1350.

C.R. Sullivan, S.R. Sanders, Microfabrication process for high-frequency power-conversion transformers, 26th Annual IEEE Power Electronics Specialists Conference, 2 (1995) 658-664.

X. Ming, T.M. Liakopoulos, C.H. Ahn, S.H. Han, H.J. Kim, A microfabricated transformers for high-frequency power or signal conversion, IEEE T. Magn., 34(2002) 1369-1371.

C.H. Ahn, Y.J. Kim, M.G. Allen, A Planar variable reluctance magnetic micromotor with fully integrated stator and coils, IEEE Microelectromech. S., 2 (1999) 165-163.

E.I. Cooper, C. Bonhote, J. Hiedmann, Y. Hsu, P. Kern, J.W. Lam, M. Ramasubramanian, N. Robertson, L.T. Romankiw, H. Xu, Recent developments in high-moment electroplated materials for recording heads, IBM J. Res. Dev., 49 (2005) 103-126.

W.Y. Lee, M.F. Toney, D. Mauri, High magneto-resistance in sputtered permalloy thin films through growth on seed layers of $(Ni_{0.81}\ Fe_{0.19})_{1-x}\ Cr_x$, IEEE T. Magn., 36 (2000) 381-385.

M. Takai, K. Kageyama, S. Takefusa, A. Nakamura, T. Osaka, Magnetic properties of electroless-deposited NiFeB and electrodeposited NiFe alloy thin films, IEICTE Trans. Electron., E78-C (1995) 1530-1535.

M. Romera, R. Ranchal, D. Ciudad, M. Maicas, C. Aroca, Magnetic properties of sputtered permalloy/molybdenum multilayers, J. Appl. Phys., 110 (2011) 083910-1-3.

J. Quemper, S. Nicolas, J.P. Gilles, Permalloy electroplating through photoresist molds, Sensor. Actuat. A: Phys., 74 (1999) 1-4.

T. O'Donnell, N. Wang, S. Kulkarni, R. Meere, F.M.F. Rhen, S. Roy, S.C. O'Mathuna, Electrodeposited anisotropic NiFe 45/55 thin films for high-frequency micro-inductor applications, J. Magn. Magn. Mater., 322 (2010) 1690-1693.

T. Yokoshima, M. Kaseda, M. Yamada, T. Nakanishi, Increasing the resistivity of electrodeposited high Bs CoNiFe thin films, IEEE T. Magn., 35 (1999) 2499-2501.

T. Yokoshima, D. Kaneko, M. Akahori, H. Nam, T. Osaka, Electroless CoNiFeB soft magnetic thin films with high corrosion resistance, J. Electroanal. Chem., 491 (2000) 197-202.

T. Yokoshima, M. Sobue, D. Kaneko, Magnetic properties of high Bs CoNiFeB soft magnetic thin film electroless deposition, Proc. 2001 Joint Int. Meeting of ECS and ISE (2001).

J.F. Rohan, B.M. Ahern, K. Reynolds, S. Crowley, D.A. Healy, F.M.F. Rhen, S. Roy, Electroless thin film CoNiFe-B alloys for integrated magnetics on Si, Electrochim. Acta, 54 (2009) 1851-1856.

Y. Zhang, G. Ding, H. Wang, B. Cai, Electroplating of low stress permalloy MEMS, Mater. Charact., 57 (2006) 121-126.

Y. Zhang, G. Ding, H. Wang, S. Fu, Low-stress permalloy for magnetic switches, IEEE T. Magn., 42 (2005) 51-55.

R. Meere, T. O'Donnell, N. Wang, N. Achotte, S. Kulkarni, S.C. Ó Mathúna, Size and performance trade-offs in micro-inductors for high frequency DC-DC converters, IEEE T. Magn., 45 (2009) 4234-4237.

R. Anthony, N. Wang, S. Kulkarni, S.C. Ó Mathúna, Advances in planar coil processing for improved microinductor performance, IEEE T. Magn., 50 (2014) 1-4.

D. Kim, R. Shanmugam, M. Choi, B. Yoo, Formation of CoNi alloy thin films on silicon by electroless deposition, Electrochim. Acta, 75 (2012) 42-48.

M. Kawamori, S. Yagi, E. Matsubara, Nickel alloying effect on formation of cobalt nanoparticles and nanowires via electroless deposition under a magnetic field, J. Electrochem. Soc., 159 (2012) E37-E44.

M. Donnabelle L. Balela, S. Yagi, E. Matsubara, Fabrication of cobalt nanowires by electroless deposition under external magnetic field, J. Electrochem. Soc., 158 (2011) D210-D216.

M. Kawamori, S. Yagi, E. Matsubara, Iron alloying effect on formation of cobalt nanoparticles and nanowires via electroless deposition under a magnetic field, J. Electrochem. Soc., 161 (2014) D59-D66.

F. Inoue, H. Philipsen, M.H. van der Veen, S. Van Huylenbroeck, S. Armini, H. Struyf, T. Tanaka, Role of bath composition in electroless Cu seeding on Cu liner for through Si vias, ECS J. Solid State Sci. Technol., 4 (2015) N3108-N3112.

J. Sudagar, J. Lian, W. Sha, Electroless nickel, alloy, composite and nano coating- A critical review, J. Alloy. Compd., 571 (2013) 183-204.

Y. Tan, K.Y. Lim, Understanding and improving the uniformity of electrodeposition, Surf. Coat. Tech., 167 (2003) 255-262.

M. Takai, S. Takefusa, T. Yokoshima, T. Osaka, Micro-Patterning of NiB Films by means of electroless plating, J. Surf. Finish. Soc., 48 (1997) 98-99.

M. Takai, S. Takefusa, T. Yokoshima, T. Osaka, Fundamental aspects of electrochemical deposition and dissolution including modelling, Proc. Electrochem. Soc., 358 (1997) PV97-27.

T. Osaka, T. Homma, K. Saito, A. Takekoshi, Y. Yamazaki, T. Namikawa, "Co-based soft magnetic films produced by electroless deposition", J. Electrochem. Soc., 139 (1992) 1311-1314.

T. Asahi, T. Yokoshima, J. Kawaji, T. Osaka, H. Ohta, M. Ohmori, H. Sakai, Novel soft magnetic underlayer for double-layered perpendicular magnetic recording media: Electroless-deposited films of CoNiFe-based alloy, IEEE T. Magn., 40 (2004) 2356-2358.

T. Osaka, T. Asahi, T. Yokoshima, J. Kawaji, Electroless-deposited soft magnetic underlayer on silicon substrate for double layered perpendicular magnetic recording media, J. Magn. Magn. Mater., 287 (2005) 292-297.

T. Xuan, L. Zhang, Q. Huang, Crystallization behaviour of electroless Co-Ni-B alloy plated in magnetic field in presence of cerium, T. Nonferr. Metal. Soc., 16 (2006) 363-367.

A. F. Schmeckenbecher, Chemical nickel-iron films, J. Electrochem. Soc., 113 (1966) 778-782.

L. Wang, L. Zhao, G. Huang, X. Yuan, B. Zhang, J. Zhang, Composition, structure and corrosion characteristics of Ni-Fe-P and Ni-Fe-P-B alloy deposits prepared by electroless plating, Surf. Coat. Tech., 126 (2000) 272-278.

S. Wang, Studies of electroless plating of Ni-Fe-P alloys and the influence of some deposition parameters on the properties of the deposits, Surf. Coat. Tech., 86 (2004) 372-376.

T. Saito, E. Sato, M. Matsoukam, C. Iwakura, Electroless deposition of Ni-B, Co-B and Ni-Co-B alloys using dimethylamineborane as reducing agent, J. Appl. Electrochem., 28 (1998) 559-563.

L. Neel, Remarks on the theory of the magnetic properties of thin layers and fine grains, J. Phys.(Paris) Radium, 17 (1956) 250-255.

I.W. Wolf, Stress-reducing organic additives in the sulphate-chloride bath for nickel-iron deposition, Electrochem. Technol., 1 (1963), 164-167.

I. Tabakovic, V. Inturi, S. Riemer, Composition, structure, stress and coercivity of electrodeposited soft magnetic CoNiFe films, J. Electrochem. Soc., 149 (2002) C18-22.

M. Saito, N. Ishiwata, K. Ohashi, Evaluation of the crystal structure, film properties, and B_s of electroplated CoNiFe films, J. Electrochem. Soc. 149 (2002) C642-C647.

J.B. Yi, X.P. Li, J. Ding, H.L. Seet, Study of the grain size, particle size and roughness of substrate in relation to the magnetic properties of electroplated permalloy, J. Alloy. Compd., 238 (2007) 230-236.

Figure legends:

Graphical Abstract: 3-D X-ray images of fabricated micromagnetic components with magnetic cores. Variable Ni and Fe alloys from similar bath and their hysteresis curves ($Ni_{81}Fe_{19}$ and $Ni_{37}Fe_{63}$).

Fig.1 Permalloy film (a) thickness versus time. Cross-sectional SEM images of $Ni_{81}Fe_{19}$ films with thicknesses (b) 770 nm and (c) 1.58 µm.

Fig.2. Influence of Ni ion concentration (keeping Ni:Fe salt same by weight) on deposition rate.

Fig.3. Influence of DMAB concentration on feasible deposition temperature.

Fig.4. Plan SEM images of electrolessly deposited films from baths with increasing DMAB concentration and decreasing temperature: (a) 0.017 mol-dm^{-3} at 85 ^{0}C. b) 0.034 mol-dm^{-3} at 75 ^{0}C. c) 0.102 mol-dm^{-3} at 65 ^{0}C. (d) 0.136 mol-dm^{-3} at 58 ^{0}C.

Fig.5. Influence of DMAB concentration on Ni and Fe content in the film.

Fig.6. Hysteresis loops of $Ni_{81}Fe_{19}$ and $Ni_{37}Fe_{63}$ films.

Fig.7. Anisotropy field and coercivity of $Ni_{81}Fe_{19}$ films deposited in the presence of magnetic field.

Fig.8. Permeability a) real part and b) imaginary part of $Ni_{81}Fe_{19}$ films deposited to the layer thickness shown at 20 Oe external bias field.

Fig.9. Electrical resistivity of thin films with varying Ni composition.

Fig.10. XRD pattern for $Ni_{81}Fe_{19}$ and $Ni_{37}Fe_{63}$ thin film deposits.

Table-I: Borane based Nickel-Iron baths. Concentrations are in mol dm^{-3}.

Bath Contents	Bath-I	Bath-II	Bath-III	Bath-IV	Bath-V
Di-ammonium Citrate	0.027	0.027	0.027	0.027	0.027

Lactic Acid	0.22	0.22	0.22	0.22	0.22
$NiSO_4$. $6H_2O$	0.060	0.060	0.060	0.060	0.060
$FeSO_4.7H_2O$	0.058	0.058	0.058	0.058	0.058
DMAB Content	0.017	0.034	0.068	0.102	0.136
pH	6.5	6.5	6.5	6.5	6.5
Temp. (^{0}C)	85	75	65	60	58
Ni and Fe composition	Ni: 81% Fe: 19%	Ni: 81% Fe: 19%	Ni: 74% Fe: 26%	Ni: 55% Fe: 45%	Ni: 37% Fe: 63%